Effects of Electrolyte Concentration and pH on the Coalescence Stability of β-Lactoglobulin Emulsions: Experiment and Interpretation

Slavka Tcholakova,[†] Nikolai D. Denkov,*[,†] Doroteya Sidzhakova,[†] Ivan B. Ivanov,[†] and Bruce Campbell[‡]

Laboratory of Chemical Physics & Engineering, Faculty of Chemistry, Sofia University, 1164 Sofia, Bulgaria, and Kraft Foods Inc., 801 Waukegan Road, Glenview, Illinois 60025, USA

Received December 16, 2004. In Final Form: March 14, 2005

Experimental results are presented about the effects of ionic strength and pH on the mean drop-size after emulsification and on the coalescence stability of emulsions, stabilized by a globular protein β-lactoglobulin (BLG). The mean drop-size is determined by optical microscopy, whereas the coalescence stability is characterized by centrifugation. In parallel experiments, the ζ-potential and protein adsorption on drop surface are determined. The experiments are performed at two different BLG concentrations, 0.02 and 0.1 wt%. The electrolyte concentration in the aqueous phase, C_{EL}, is varied between 1.5 mM and 1 M, and pH is varied between 4.0 and 7.0. The experiments show that the mean drop-size after emulsification depends slightly on C_{EL}, at fixed protein concentration and natural pH = 6.2. When pH is varied, the mean drop-size passes through a maximum at fixed protein and electrolyte concentrations. A monolayer protein adsorption is registered in the studied ranges of C_{EL} and pH at low BLG concentration of 0.02 wt%. In contrast, a protein multilayer is formed at higher BLG concentration, 0.1 wt%, above a certain electrolyte concentration (C_{EL} > 100 mM, natural pH). The experimental results for the emulsion coalescence stability are analyzed by considering the surface forces acting between the emulsion drops. The electrostatic, van der Waals, and steric interactions are taken into account to calculate the barriers in the disjoining pressure isotherm at the various experimental conditions studied. The comparison of the theoretically calculated and the experimentally determined coalescence barriers shows that three qualitatively different cases can be distinguished. (1) Electrostatically stabilized emulsions, with monolayer protein adsorption, whose stability can be described by the DLVO theory. (2) Sterically stabilized emulsions, in which the drop−drop repulsion is created mainly by overlapping protein adsorption multilayers. A simple theoretical model is shown to describe emulsion stability in these systems. (3) Sterically stabilized emulsions with a monolayer adsorption on drop surface.

1. Introduction

Proteins are widely used as emulsifiers in food, cosmetic, and pharmaceutical industries. The efficiency of protein emulsifiers depends on various factors, such as protein concentration and adsorption, drop size, electrolyte concentration, pH, and thermal treatment.[1−18] The effects of these factors on coalescence stability are still poorly understood. As an example, it is often assumed, and in some studies it was experimentally found, that higher protein adsorption leads to more stable emulsions (e.g., refs 1−3,14). However, published experimental results evidence that this correlation is not always true—when

* Author to whom correspondence should be addressed. Laboratory of Chemical Physics & Engineering, Faculty of Chemistry, Sofia University, 1 James Bourchier Ave., 1164 Sofia, Bulgaria, Phone: (+359-2) 962 5310. Fax: (+359-2) 962 5643. E-mail: nd@lcpe.uni-sofia.bg.

† Sofia University.

‡ Kraft Foods, Inc.

(1) Graham, D. E.; Phillips, M. C. The conformation of proteins at interfaces and their role in stabilizing emulsions. In *Theory and Practice of Emulsion Technology*; Smith, A. L., Ed.; Academic Press: New York, 1976; p 75.

(2) Phillips, M. C. Protein conformation at liquid interfaces and its role in stabilizing emulsions and foams. *Food Techn.* **1981**, *1*, 50.

(3) Van Aken, G. A.; Zoet, F. D. Coalescence in highly concentrated emulsions. *Langmuir* **2000**, *16*, 7131.

(4) Das, K. P.; Kinsella, J. E. Droplet size and coalescence stability of whey protein stabilized milkfat peanut oil emulsions. *J. Food Sci.* **1993**, *58*, 439.

(5) Das, K. P.; Kinsella, J. E. Stability of food emulsions: physicochemical role of protein and nonprotein emulsifiers. *Adv. Food Nutr. Res.* **1990**, *34*, 81.

(6) Das, K. P.; Kinsella, J. E. pH dependent emulsifying properties of β-lactoglobulin. *J. Dispersion Sci. Technol.* **1989**, *10*, 77.

(7) Van Aken, G. A.; van Vliet, T. Mechanism of coalescence in highly concentrated protein-stabilized emulsions. In *Food Colloids 2000, Fundamentals of Formulation*; Dickinson, E., Miller, R., Eds.; Royal Society of Chemistry: Cambridge, 2001; p 125.

(8) Das K. P.; Kinsella, J. E. Effect of heat denaturation on the adsorption of β-lactoglobulin at the oil/water interface and on the coalescence stability of emulsions. *J. Colloid Interface Sci.* **1990**, *139*, 551.

(9) Dickinson, E. Proteins at interfaces and in emulsions. Stability, rheology and interactions. *J. Chem. Soc., Faraday Trans.* **1998**, *94*, 1657.

(10) Van Aken, G. A.; van Vliet, T. Flow-induced coalescence in protein-stabilized highly concentrated emulsions: Role of shear-resisting connections between the droplets. *Langmuir* **2002**, *18*, 7364.

(11) Kim, H.-J.; Decker, E. A.; McClements, D. J. Effect of cosolvents on thermal stability of globular protein-stabilized emulsions. In *Third World Congress on Emulsions,* Lyon **2002**, Reference 035.

(12) Kulmyrzaeva, A. A.; Schubert, H. Influence of KCl on the physicochemical properties of whey protein stabilized emulsions. *Food Hydrocolloids* **2004**, *18*, 13.

(13) Sliwinski, E. L.; Roubos, P. J.; Zoet, F. D.; van Boekel, M. A. J. S.; Wouters, J. T. M. Effects of heat on physicochemical properties of whey-protein stabilized emulsions. *Colloids Surf.* **2003**, *31*, 231.

(14) Tcholakova, S.; Denkov, N. D.; Ivanov, I. B.; Campbell, B. Coalescence in β-lactoglobulin-stabilized emulsions: effects of protein adsorption and drop size. *Langmuir* **2002**, *18*, 8960.

(15) Tcholakova, S.; Denkov, N. D.; Ivanov, I. B.; Campbell, B. Coalescence in protein stabilized emulsions. In *Third World Congress on Emulsions,* Lyon **2002**, Paper No. 200.

(16) Kim, H.-J.; Decker, E. A.; McClements, D. J. Impact of protein surface denaturation on droplet flocculation in hexadecane oil-in-water emulsions stabilized by beta-lactoglobulin. *J. Agric. Food Chem.* **2002**, 50, 7131−7137.

(17) Kim, H.-J.; Decker, E. A.; McClements, D. J. Role of postadsorption conformation changes of beta-lactoglobulin on its ability to stabilize oil droplets against flocculation during heating at neutral pH. *Langmuir* **2002**, *18*, 7577−7583. 3

(18) Kulmyrzaev, A.; Bryant, C.; McClements, D. J. Influence of sucrose on the thermal denaturation, gelation, and emulsion stabilization of whey proteins. *J. Agric. Food Chem.* **2000**, *48*, 1593.

10.1021/la046891w CCC: $30.25
Published on Web 04/08/2005

pH of the protein solution is varied, protein adsorption is found to be maximal,[5,6,19−21] whereas emulsion stability is often minimal[1,5,6,22] around the protein isoelectric point (IEP) with all other conditions being fixed. Therefore, the relation between protein adsorption and coalescence stability of emulsions (both depending on pH, electrolyte concentration, and other factors) deserves further investigation.

A major problem in the analysis of the effects of various factors on coalescence stability of emulsions is created by the fact that the molecular mechanism of protein stabilization is still rather obscure.[23−25] In some studies, the ability of protein emulsifiers to prevent drop−drop coalescence is explained by the formation of viscoelastic adsorption layers, which are assumed to stabilize very efficiently the emulsion films between neighboring drops.[1,9,25] For this reason, the rheological properties of protein adsorption layers are often discussed in relation to emulsion stability.[1,2,9,25−30] However, a clear picture about the mechanism of film rupture and of the respective molecular mechanism of emulsion stabilization by proteins is missing. Furthermore, recent experimental results[15] showed that the aging (shelf-storage at room temperature) and the thermal treatment of emulsions, stabilized by BLG, lead to opposite effects on the emulsion coalescence stability (the aging decreases, whereas the heating strongly increases emulsion stability), although both treatments are known to increase the elasticity of BLG adsorption layers.[30] The latter example shows that the relationship between the viscoelastic properties of protein adsorption layers and emulsion stability is far from being straightforward.

In other studies, the stability of protein emulsions is explained by considering the colloidal surface forces, which act in the emulsion films between neighboring drops.[12,22] van der Waals, electrostatic, and steric interactions are expected to play a significant role in these systems.[12,22,31−35] The stabilizing role of the adsorbed protein molecules is, therefore, explained with their effect on the surface forces, e.g., by modifying the electrical potential of drop surface[12,22] and the van der Waals interactions,[36,37] and by creating a steric barrier to drop−drop coalescence.[22,31,35] In other words, it is assumed in these studies that the main role of the adsorbed protein is to modify the disjoining pressure, Π (force per unit area), which in turn determines the stability of the emulsion films.

Whatever is the mechanism of emulsion stabilization by protein molecules (building up a viscoelastic adsorption layer or creating a significant surface force barrier to coalescence), the amount of adsorbed protein and the structure of the adsorption layer should play a very significant role in emulsion stability. In previous studies,[14,15] we quantified the coalescence stability of BLG-containing emulsions by measuring the critical osmotic pressure, which leads to drop coalescence and emulsion destruction, P_{OSM}^{CR}. The classical method of emulsion centrifugation was appropriately modified to measure P_{OSM}^{CR}, which can be used as a convenient quantitative measure of the emulsion coalescence stability.[14,15] In parallel experiments, protein adsorption on the surface of the emulsion drops was determined. The results demonstrated[14,15] that P_{OSM}^{CR} increases with protein adsorption, Γ, and a large step of P_{OSM}^{CR} was observed at a threshold value, Γ*, almost equal to the adsorption in a dense monolayer, Γ_M. The experiments in refs 14 and 15 were performed at fixed pH = 6.2 and electrolyte concentration, C_{EL} = 150 mM.

The current study presents new experimental results, obtained at various electrolyte concentrations (between 1.5 mM and 1 M) and pH values (between 4.0 and 7.0). The experiments are made at two BLG concentrations, 0.02 and 0.1 wt%, which are chosen to correspond to monolayer and multilayer protein adsorption, respectively, at natural pH = 6.2 and 150 mM NaCl.[14] The critical osmotic pressure for coalescence, P_{OSM}^{CR}; protein adsorption, Γ; mean drop-size, d_{32}; and ζ-potential of the emulsion drops are measured. The experimental results for the coalescence stability of the studied emulsions are compared with theoretical estimates of the barriers in the disjoining pressure isotherm, Π_{MAX}, which take into account the van der Waals, electrostatic, and steric forces between the emulsion droplets. The analysis reveals that three qualitatively different cases can be distinguished. (1) Electrostatically stabilized emulsions with monolayer protein adsorption. (2) Sterically stabilized emulsions, in which drop−drop repulsion is caused mainly by overlapping protein adsorption multilayers. (3) Sterically stabilized emulsions with a monolayer adsorption on drop surface. In each of these cases, a specific group of factors is expected to control emulsion stability.

2. Materials and Methods

2.1. Materials. β-Lactoglobulin (BLG) from bovine milk was used as received from Sigma (catalog no. L-0130, lot no. 052K7018). Commercial-grade soybean oil was purified from polar

(19) Atkinson, P. J.; Dickinson, E.; Horne, D. S.; Richardson, R. Neutron reflectivity of adsorbed β-casein and β-lactoglobulin at the air/water interface. *J. Chem. Soc., Faraday Trans.* **1995**, *91*, 2847.

(20) Lu, J. R.; Su, T. J.; Thomas, R. K. Structural conformation of bovine serum albumin layers at the air−water interface studied by neutron reflection. *J. Colloid Interface Sci.* **1999**, *213*, 426.

(21) Benjamins, J. Static and dynamic properties of proteins adsorbed at liquid interfaces. Ph.D. Thesis, Wageningen University, 2000.

(22) Narsimhan, G. Maximum disjoining pressure in protein stabilized concentrated oil-in-water emulsions. *Colloids Surf.* **1992**, *62*, 41.

(23) Dalglish, D. G. Food emulsions stabilized by proteins. *Curr. Opin. Colloid Interface Sci.* **1997**, *2*, 573.

(24) Van Aken, G. A.; Blijdenstein, T. B. J.; Hotrum, N. E. Colloidal destabilisation mechanisms in protein-stabilised emulsions. *Curr. Opin. Colloid Interface Sci.* **2003**, *4*, 371.

(25) Izmailova, V. N.; Yampolskaya, G. P. Rheological parameters of protein interfacial layers as a criterion of the transition from stable emulsions to microemulsions. *Adv. Colloid Interface Sci.* **2000**, *88*, 99.

(26) Martin, A.; Bos, M.; Stuart, M. C.; van Vliet, T. Stress−strain curves of adsorbed protein layers at the air/water interface measured with surface shear rheology. *Langmuir* **2002**, *18*, 1238.

(27) Murray, B. Interfacial rheology of food emulsifiers and proteins. *Curr. Opin. Colloid Interface Sci.* **2002**, *7*, 426.

(28) Petkov, J. T.; Gurkov, T. D.; Campbell, B.; Borwankar R. P. Dilatational and shear elasticity of gellike protein layers on air−water interface. *Langmuir* **2000**, *16*, 3703.

(29) Murray, B. S.; Cattin, B.; Schuler, E.; Sonmez, Z. O. Response of adsorbed protein films to rapid expansion. *Langmuir*, **2002**, *18*, 9476.

(30) Roth, S.; Murray, B. S.; Dickinson, E. Interfacial shear rheology of aged and heat-treated β-lactoglobulin films: Displacement by nonionic surfactant. *J. Agric. Food Chem.* **2000**, *48*, 1491.

(31) Dimitrova, T. D.; Leal-Calderon, F.; Gurkov, T. D.; Campbell, B. Disjoining pressure vs thickness isotherms of thin emulsion films stabilized by proteins. *Langmuir* **2001**, *17*, 8069.

(32) Cascao Pereira, L. G.; Johansson, Ch.; Radke, C. J.; Blanch, H. Surface forces and drainage kinetics of protein-stabilized aqueous films. *Langmuir* **2003**, *19*, 7503.

(33) Claesson, P. M.; Blomberg, E.; Froberg, J. C.; Nylander, T.; Arnebrant, T. Protein interactions at solid surfaces. *Adv. Colloid Interface Sci.* **1995**, *57*, 161.

(34) Dimitrova, T. D.; Leal-Calderon, F. Rheological properties of highly concentrated protein-stabilized emulsions. *Adv. Colloid Interface Sci.* **2004**, *108*, 49.

(35) Dimitrova, T. D.; Leal-Calderon, F.; Gurkov, T. D.; Campbell, B. Surface forces in model oil-in-water emulsions stabilized by proteins. *Adv. Colloid Interface Sci.* **2004**, *108*, 73.

(36) Tcholakova, S.; Denkov, N. D.; Borwankar, R.; Campbell, B. van der Waals Interaction between Two Truncated Spheres Covered by a Uniform Layer (Deformed Drops, Vesicles, Bubbles). *Langmuir* **2001**, *17*, 2357.

(37) Roth, C. M.; Neal, B. L.; Lenhoff, A. M. van der Waals interactions involving proteins. *Biophys. J.* **1996**, *70*, 977.

contaminants by multiple passes through a glass column, filled with Florisil adsorbent.[38] The surface tension of purified oil was 29.5 ± 0.5 mN/m.

Protein solutions were prepared with deionized water, purified by a Milli-Q Organex system (Millipore). These solutions always contained 0.01 wt% of the antibacterial agent NaN_3 (Riedel-de Haën). The solution ionic strength was adjusted between 1.5 mM (only NaN_3) and 1 M, by using NaCl. The desired pH value was adjusted by addition of small aliquots of 0.1 M NaOH or 0.1 M HCl into the protein solution. In several series of experiments, no acid or base was added to the protein solutions and the respective "natural" pH of these solutions was equal to 6.2 ± 0.1. No protein precipitation was observed in any of the studied solutions (including those prepared at the IEP of the protein).

2.2. Emulsion Preparation. Oil-in-water emulsions were prepared by stirring for 3 min a solution of 35 mL of protein and 15 mL of soybean oil (30 vol%) with a rotor-stator homogenizer Ultra Turrax T25 (Janke & Kunkel GmbH & Co, IKA-Labortechnik), operating at 13 500 rpm.

2.3. Determination of Mean Drop-Size. The mean drop-size in the studied emulsions was determined by optical microscopy. Specimens were taken immediately after emulsion preparation. The oil drops were observed in transmitted light with microscope Axioplan (Zeiss, Germany), equipped with objective Epiplan, ×50, and connected to a CCD camera (Sony) and VCR (Samsung SV-4000). The diameters of oil drops were afterward measured (one by one) from the recorded video-frames, by using custom-made image analysis software, operating with Targa+ graphic board (Truevision, USA). The diameters of at least 10 000 drops from two to five independently prepared emulsions were measured for each system.

The mean volume-surface diameter, d_{32}, was calculated from the measured drop diameters by using the relation:

$$d_{32} = \frac{\sum_i N_i d_i^3}{\sum_i N_i d_i^2} \tag{1}$$

where N_i is the number of drops with diameter d_i. One can calculate the specific surface area of the drops, S (area per unit volume of oil), from d_{32} by the equation

$$S = \frac{\pi {d_{32}}^2}{(\pi/6){d_{32}}^3} = \frac{6}{d_{32}} \tag{2}$$

If d_{32} is expressed in micrometers, S has a dimension of square meters per milliLiter of oil.

2.4. Determination of the Protein Adsorption. Protein adsorption on the surface of the emulsion drops, Γ, was determined from the specific surface area of the drops, S, and from the decrease of the protein concentration in the aqueous phase, as a result of the emulsification process. The following mass balance, relating Γ with the decrease of the protein concentration, was used

$$\Gamma = \frac{V_C(C_{BLG}^{INI} - C_{BLG}^{SER})}{SV_{OIL}} = \frac{(1-\Phi)d_{32}}{6\Phi}(C_{BLG}^{INI} - C_{BLG}^{SER}) \tag{3}$$

where V_C and V_{OIL} are the volumes of the continuous and oil phases, Φ is the oil volume fraction, C_{BLG}^{INI} is the initial BLG concentration in the aqueous solution, and C_{BLG}^{SER} is the BLG concentration in the aqueous phase (in the serum) after emulsification. The protein concentration in the serum was determined by the method of Bradford[39]—see ref 14 for the experimental procedure.

(38) Gaonkar, A. G.; Borwankar, R. P. Competitive adsorption of monoglycerides and lecithin at the vegetable oil-water interface. *Colloids Surf.* **1991**, *59*, 331.

(39) Bradford, M. A rapid and sensitive method for the quantitation of microgram quantities of protein utilizing the principle of protein-dye binding. *Anal. Biochem.* **1976**, *72*, 248.

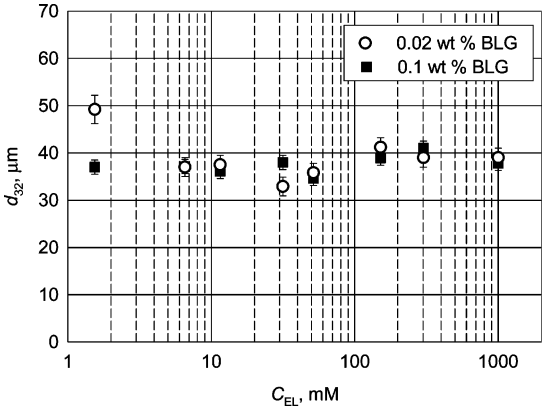

Figure 1. Mean volume-surface diameter, d_{32}, as a function of electrolyte concentration, C_{EL}, for emulsions stabilized by 0.02 wt% BLG (open circles) and 0.1 wt% BLG (filled squares); pH = 6.2 (natural).

2.5. Evaluation of the Emulsion Stability by Centrifugation. The studied emulsions were centrifuged at 20 °C in a 3K15 centrifuge (Sigma Laborzentrifugen, Germany). Preliminary experimental checks performed at different durations of the centrifugation time (ranging from 30 min up to 6 h) showed that 30 min is sufficient for completion of the process of water drainage from the emulsion cream and for reaching mechanical equilibrium at given acceleration. Therefore, all emulsions in the systematic series of experiments were centrifuged for 1 h at given acceleration. The emulsion stability was characterized by the critical osmotic pressure, P_{OSM}^{CR}, at which continuous oil layer was released on top of the emulsion cream in the centrifuge tube.[14,15] P_{OSM}^{CR} was calculated from the experimental data by using the equation:[14,15]

$$P_{OSM}^{CR} = \Delta\rho g_k (V_{OIL} - V_{REL})/A \tag{4}$$

where $\Delta\rho$ is the difference between the mass densities of the aqueous and oil phases, g_k is the centrifugal acceleration, V_{OIL} is the total volume of oil used for emulsion preparation, V_{REL} is the volume of released oil at the end of centrifugation, and A is the cross-sectional area of the centrifuge test tube. Equation 4 implies that P_{OSM}^{CR} is the osmotic pressure of the emulsion at the top of the emulsion column, where the latter is in mechanical equilibrium with the continuous layer of released oil. The principle of the method and the used procedures are described in ref 14.

2.6. ζ-Potential Measurements. The ζ-potential of the oil−water interface was determined by measuring the electrophoretic mobility of oil drops dispersed in aqueous solution of desired pH and electrolyte concentration. The measurements were carried out on Zetasizer II C equipment (Malvern Instruments, Ltd). The Smoluchowki equation was used to calculate the ζ-potential from the electrophoretic mobility because $\kappa d_{32} \gg 1$ in all systems (κ is the inverse Debye length).

2.7. Interfacial Tension. The oil−water interfacial tension was measured by applying the drop-shape analysis to pendant oil drops. The measurements were performed at 23.5 ± 0.5 °C on a Drop Shape Analysis System DSA 10 (Krüss GmbH, Hamburg, Germany).

3. Experimental Results and Discussion

In the current section, we present the main experimental results and their qualitative explanations. Quantitative interpretation of the data about emulsion coalescence stability is presented in Section 4, by considering the surface forces acting between the drops.

3.1. Mean Drop-Size after Emulsification. The dependence of mean drop-size, d_{32}, on electrolyte concentration, C_{EL}, is presented in Figure 1 for BLG concentrations of 0.02 and 0.1 wt%. At both BLG concentrations, d_{32} remains almost constant, 38 ± 4 μm, at $C_{EL} \geq 5$ mM.

At low BLG and electrolyte concentrations, $C_{BLG} = 0.02$ wt% and $C_{EL} = 1.5$ mM, d_{32} is somewhat larger, 49 ± 3 μm.

The observation that d_{32} is almost the same for both studied protein concentrations (at $C_{EL} > 5$ mM) means that the kinetics of protein adsorption does not play a significant role under these emulsification conditions. Otherwise, one could expect that the mean drop-size would be smaller at the higher protein concentration, at which faster adsorption should occur. The only exception is the result at the lowest electrolyte concentration, $C_{EL} = 1.5$ mM, at which d_{32} is larger at 0.02 wt% BLG, as compared to 0.1 wt% BLG (49 vs 37 μm). This difference could be related to a slower protein adsorption, at 0.02 wt% BLG, due to a long-range electrostatic repulsion between the protein molecules and the oil−water interface at this low electrolyte concentration.[32]

The fact that d_{32} is almost constant in the entire range of electrolyte concentrations at pH = 6.2 for the emulsions prepared at $C_{BLG} = 0.1$ wt% suggests that the effect of drop−drop coalescence on the mean drop size during emulsification is negligible. Otherwise, one could expect that the significant change in the interdroplet electrostatic interactions, with the variation of C_{EL}, would affect the coalescence probability and, hence, the mean drop size.[40−44]

In general, the variations in d_{32}, at fixed oil viscosity and fixed intensity of stirring during emulsification, can be explained by considering two different types of factors: (1) interfacial tension, which affects the drop breakage process, and (2) factors affecting the drop−drop coalescence during emulsification.[40−44] At high emulsifier concentrations (in the so-called "surfactant-rich regime"), the drop−drop coalescence is usually negligible and the mean drop-size is well described by the Kolmogorov−Hinze theory of emulsification:[45,46]

$$d_K \sim \epsilon^{-2/5} \sigma_{OW}^{3/5} \rho_C^{-1/5} \quad (5)$$

where d_K is the maximal drop-size in the absence of coalescence (shown by us[43,44] to be approximately equal to d_{32} for soybean oil-in-water emulsions), ρ_C is the mass density of the continuous phase, and ϵ is the average density of power dissipation (rate of energy dissipation per unit volume) in the head of the emulsification device. In the presence of significant drop−drop coalescence, the mean drop-size could be significantly larger than d_K, as estimated by eq 5.[41−44]

Let us explain now the observed larger value of d_{32} at $C_{BLG} = 0.02$ wt% and $C_{EL} = 1.5$ mM. To check whether this larger value is due to higher interfacial tension (see eq 5), we measured the interfacial tensions at $C_{EL} \approx 1.5$ mM ($\sigma_{OW} = 27$ mN/m) and at $C_{EL} \approx 150$ mM ($\sigma_{OW} = 18.7$ mN/m). From eq 5 and the measured values of σ_{OW}, one can estimate the expected effect of the interfacial tension variation on the mean drop-size, at negligible contribution of drop−drop coalescence. Equation 5 predicts that the mean drop-size should increase by a factor of 1.25 when σ_{OW} increases from 18.7 mN/m (at 150 mM NaCl) to 27 mN/m (at 1.5 mM NaCl), which is in a good agreement with the experimental results for d_{32} at these electrolyte concentrations (41 vs 49 μm). Hence, the most probable reason for the larger drop size at $C_{EL} = 1.5$ mM is the higher interfacial tension. Thus, we can conclude that the effect of drop−drop coalescence on d_{32} is not important under these emulsification conditions (pH = 6.2).

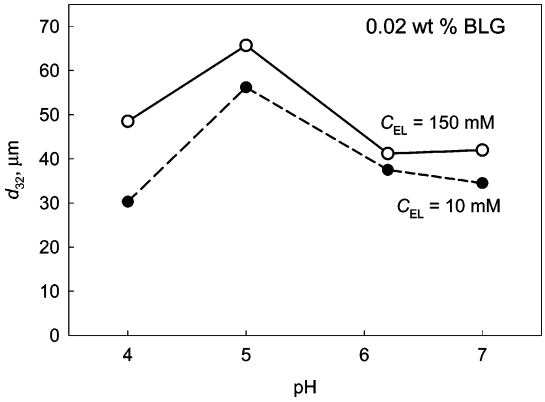

Figure 2. Mean volume-surface diameter, d_{32}, as a function of pH for emulsions stabilized by 0.02 wt% BLG at $C_{EL} = 10$ mM (filled circles) and $C_{EL} = 150$ mM (open circles).

In another series of experiments, we studied the effect of pH on d_{32} for emulsions stabilized by $C_{BLG} = 0.02$ wt% at $C_{EL} = 10$ and 150 mM. The obtained dependence of d_{32} on pH is plotted in Figure 2. One sees that d_{32} passes through a maximum for both electrolyte concentrations studied. Maximal drop size is observed at pH = 5.0, which is around the isoelectric point of the BLG molecules.[5,6,12] The value of d_{32} measured at pH = 5.0 is by a factor of 1.5 larger than that at natural pH = 6.2 (56 vs 38 μm at C_{EL} = 10 mM and 66 vs 41 μm at C_{EL} = 150 mM). At C_{EL} = 150 mM, the mean drop-size at pH = 4.0 is smaller than that at pH = 5.0 (49 vs 66 μm), but it is still larger than the one at natural pH = 6.2 (49 vs 41 μm). At lower electrolyte concentration, C_{EL} = 10 mM, the opposite trend is observed—the mean drop size at pH = 4.0 is smaller than that at natural pH (30 vs 38 μm).

As explained above, at negligible contribution of drop−drop coalescence (viz., in the surfactant-rich regime), only variations in the interfacial tension could be used to explain changes in the mean drop-size. However, the values of the interfacial tension determined at pH = 5.0 and 6.2 were the same in the framework of our experimental accuracy (18.7 ± 0.2 mN/m, measured 1 min after drop formation; $C_{EL} = 150$ mM). The kinetics of the interfacial tension, measured by drop-shape analysis of pendant oil drops in protein solutions, was also very similar in these two systems during the entire period of measurements (between 1 min and 1 h after drop formation). Thus, the Kolmogorov−Hinze model, eq 5, would predict similar mean drop-size at pH 5.0 and 6.2, which contradicts the experimental results shown in Figure 2. Therefore, the variations in the interfacial tension could not explain the observed pH dependence of d_{32}. The most probable explanation of these results is that the drop−drop coalescence plays a very significant role around the IEP and leads to larger mean drop-size.

The higher probability for drop coalescence around the IEP could be due to suppressed electrostatic repulsion between the drops and/or to structural changes in the

(40) Narsimhan, G.; Goel, P. Drop coalescence during emulsion formation in a high-pressure homogenizer for tetradecane-in-water emulsion stabilized by sodium dodecyl sulfate. *J. Colloid Interface Sci.* **2001**, *238*, 420.

(41) Walstra, P. Formation of emulsions. In *Encyclopedia of Emulsion Technology*; Marcel Dekker: New York, 1983; Chapter 2.

(42) Danner, T.; Schubert, H. Coalescence processes in emulsions. In *Food Colloids 2000, Fundamentals of Formulation*; Dickinson, E., Miller, R., Eds.; Royal Society of Chemistry: Cambridge, 2001; p 116.

(43) Tcholakova, S.; Denkov, N. D.; Danner, T. Role of surfactant type and concentration for the mean drop size during emulsification in turbulent flow. *Langmuir* **2004**, *20*, 7444.

(44) Tcholakova, S.; Denkov, N. D.; Sidzhakova, D.; Ivanov, I. B.; Campbell, B. Interrelation between drop size and protein adsorption at various emulsification conditions. *Langmuir* **2003**, *19*, 5640.

(45) Hinze, J. O. Fundamentals of the hydrodynamic mechanism of splitting in dispersion processes. *AIChE J.* **1955**, *3*, 289.

(46) Kolmogoroff, A. N. Drop breakage in turbulent flow. *C. R. Acad. Sci. URSS* **1949**, *66*, 825 (in Russian).

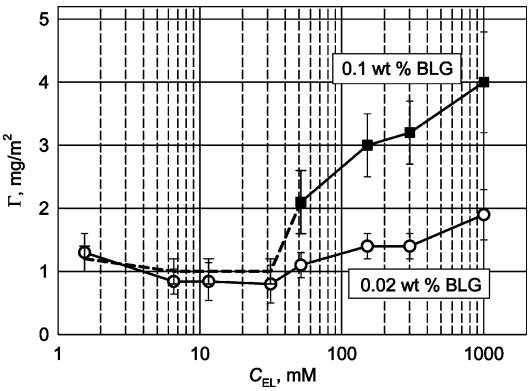

Figure 3. Protein adsorption, Γ, as a function of electrolyte concentration, C_{EL}, for emulsions stabilized by 0.02 wt% BLG (open circles) and 0.1 wt% BLG (filled squares); pH = 6.2 (natural).

protein adsorption layers, which affect the stability of the emulsion films. If we assume that the observed pH dependence is related to variations in the electrostatic repulsion only, one could expect that the results around the IEP (uncharged drop surface) would be similar to those obtained at very high electrolyte concentrations (completely screened electrostatic repulsion; see Section 4.3 for theoretical estimates of the electrostatic interaction between the drops). However, we obtained much larger drops with $d_{32} = 66$ μm at pH = IEP = 5.0, whereas $d_{32} = 39$ μm was measured at natural pH = 6.2 and $C_{EL} = 1$ M (when the electrostatic repulsion is completely suppressed). Therefore, the variations in the electrostatic interactions between the drops are insufficient to explain the observed pH dependence. This qualitative analysis of the experimental data indicates that there is a significant change in the structure of the protein adsorption layer around the IEP, which leads to inefficient steric stabilization of the emulsion films.

In conclusion, the mean drop size, d_{32}, slightly depends on C_{EL} for emulsions prepared at natural pH and is practically the same at both BLG concentrations studied (0.02 and 0.1 wt%). The effect on d_{32} at pH = 5.0 ≈ IEP is stronger due to suppressed electrostatic repulsion and ineffective steric repulsion, which lead to drop−drop coalescence during emulsification.

3.2. Protein Adsorption. The effect of C_{EL} on protein adsorption, Γ, was studied for 0.02 and 0.1 wt% BLG at natural pH = 6.2 (see Figure 3). For emulsions stabilized by 0.02 wt% BLG (open circles in Figure 3), Γ ≈ 0.8 mg/m^2 remains almost constant when C_{EL} is varied between 5 and 30 mM, followed by a gradual increase up to 1.9 mg/m^2 upon the further increase of C_{EL} to 1 M. The lower value of Γ at moderate electrolyte concentrations (between 5 and 30 mM), in comparison with the values at high electrolyte concentrations, $C_{EL} > 50$ mM, is probably due to stronger electrostatic repulsion between the protein molecules in the adsorption layer and/or more enhanced molecular unfolding upon adsorption. The screened electrostatic repulsion at high electrolyte concentrations leads to more compact adsorption layers and higher values of Γ.[21,47]

Our efforts to determine experimentally Γ in the emulsions, stabilized by 0.1 wt% BLG, were unsuccessful for C_{EL} between 1 and 30 mM. The difference between protein concentrations in the initial solution and in the serum after emulsification was within the experimental accuracy (±5%), and we could not use eq 3 to determine Γ. An estimate, by using eq 3, shows that this undetectable difference between C_{BLG}^{INI} and C_{BLG}^{SER} corresponds to Γ < 1.2 mg/m^2. Since the protein adsorption at 0.1 wt% BLG is expected to be equal or larger than the adsorption at 0.02 wt% BLG (Γ ≈ 0.8 mg/m^2), one can conclude that the value of Γ at 0.1 wt% BLG and C_{EL} between 1 and 30 mM is between 0.8 and 1.2 mg/m^2 (this estimate is indicated by the dashed curve in Figure 3).

At higher electrolyte concentration, 50 mM ≤ C_{EL} ≤ 1 M, the protein adsorption was found to increase from 2.1 up to 4.0 mg/m^2 at $C_{BLG} = 0.1$ wt% (filled squares in Figure 3). In this range of electrolyte concentrations, the protein adsorption at 0.1 wt% BLG is much higher in comparison with that at 0.02 wt% BLG, which is due to formation of adsorption multilayers (theoretical estimates and experimental results verifying this hypotheses are described in the following paragraphs). Indeed, in our previous study,[14] we proved that an adsorption multilayer is formed at $C_{BLG} = 0.1$ wt% and $C_{EL} = 150$ mM.

The theoretical estimate of the maximal adsorption in a monolayer of intact spherical molecules of BLG gives $\Gamma_{M,Int} = 2.75$ mg/m^2. For this estimate, we used the diameter, 3.58 nm, and molecular mass, 18 400 g/mol, of intact BLG molecules, as cited in the literature.[48] The estimate of $\Gamma_{M,Int}$ is based on the assumption that the molecules are closely packed in a hexagonal 2D-array and thus occupy 90.7% of the surface.[49] Note that the measured values of Γ at $C_{BLG} = 0.1$ wt% and $C_{EL} > 150$ mM are higher than $\Gamma_{M,Int}$, which is a direct proof that a protein adsorption multilayer is formed on the drop surface at these high protein and electrolyte concentrations. In contrast, the adsorption monolayer, with Γ < 1.2 mg/m^2, is formed at lower electrolyte concentration, $C_{EL} < 50$ mM NaCl, due to a significant electrostatic repulsion between the charged protein molecules.

As shown in the literature,[1,2,5,6] two types of molecules can be distinguished in the protein adsorption multilayers. The molecules in the first adsorption layer, which is in direct contact with the oil−water interface, are irreversibly adsorbed on the drop surface. In contrast, the molecules adsorbed over the first layer are reversibly adsorbed and could be rinsed by replacing the emulsion serum (which is in equilibrium with the adsorption multiplayer) with an electrolyte solution deprived of protein.[14,44] The process of protein rinse from the drop surface presents, in fact, a desorption of the protein molecules, which are not in direct contact with the oil−water interface, due to their lower adsorption energy (as compared to the adsorption energy of the molecules in the first adsorption layer).

To check additionally whether the measured high protein adsorption at 0.1 wt% BLG and high electrolyte concentration is due to formation of a multilayer, we rinsed the emulsion formed at $C_{EL} = 1$ M (Γ = 4.0 mg/m^2, Figure 3) with 1 M NaCl solution. The following procedure was used.[14] First, the original emulsion was stored undisturbed for 1 h and a cream of closely packed drops formed in the upper part of the emulsion under the effect of gravity. Afterward, by using a syringe, the serum remaining below the cream was removed and replaced by the same volume of 1 M NaCl and 0.1 wt% NaN_3 solution (without dissolved

(47) Cho, D.; Narsimhan, G.; Franses, E. I. Adsorption dynamics of native and pentylated bovine serum albumin at air−water interfaces: Surface concentration/surface pressure measurements. *J. Colloid Interface Sci.* **1997**, *191*, 312.

(48) Cornec, M.; Cho, D.; Narsimhan, G. Adsorption dynamics of α-Lactalbumin and β-Lactoglobulin at air−water interfaces. *J. Colloid Interface Sci.* **1999**, *214*, 129.

(49) Princen, H. M. The structure, mechanics, and rheology of concentrated emulsions and fluid foams. In *Encyclopedea of Emulsion Science and Technology*; Söblom, J., Ed.; Marcel Dekker: New York, 2001; Chapter 11.

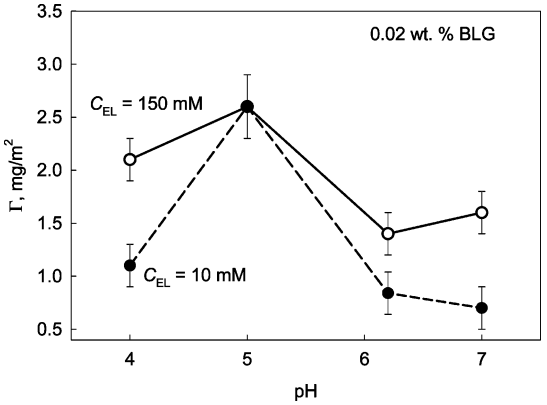

Figure 4. Protein adsorption, Γ, as a function of pH, for emulsions stabilized by 0.02 wt% BLG at $C_{EL} = 10$ mM (filled circles) and $C_{EL} = 150$ mM (open circles).

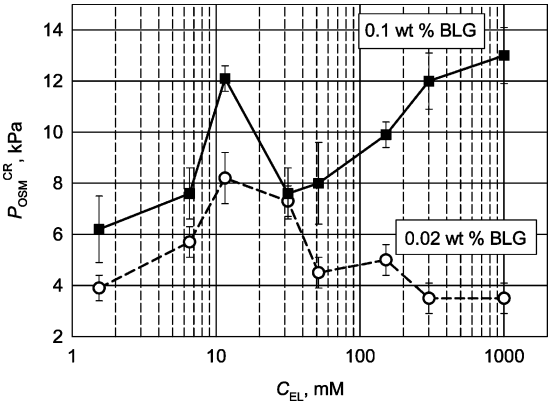

Figure 5. Critical osmotic pressure for coalescence, P_{OSM}^{CR}, as a function of electrolyte concentration, C_{EL}, in emulsions stabilized by 0.02 wt% BLG (open circles) and 0.1 wt% BLG (filled squares); pH = 6.2 (natural).

protein). This sample was gently agitated by hand until the emulsion drops completely dispersed in the entire volume and then was left undistributed for another 1 h. A sample from the rinsing electrolyte solution, which remained below the cream, was taken, and the protein concentration was determined by the method of Bradford.[39] By applying a mass balance for the protein used in emulsion preparation, from the average drop size, d_{32}, and from the protein concentrations in the initial solution, C_{BLG}^{INI}, in the serum after emulsification, C_{BLG}^{SER}, and in the rinsing solution, C_{BLG}^{RIN}, we calculated the protein adsorption before and after rinsing of the cream. We found that the initial adsorption of 4.0 mg/m² decreased down to 2.6 mg/m² as a result of rinsing. A second and third rinsing procedure applied on the same emulsion did not lead to further significant desorption of protein. This experimental result confirms our assumption that a second adsorption layer of reversibly bound protein molecules is built on the drop surfaces at electrolyte concentrations above ca. 0.1 M NaCl at $C_{BLG} = 0.1$ wt%. Note that the protein adsorption after rinsing, 2.6 mg/m², is close to the one corresponding to a close-packed monolayer of BLG molecules, $\Gamma_{M,Int} = 2.75$ mg/m².

Similarly, the rinsing procedure was applied to emulsions prepared with $C_{BLG} = 0.02$ wt% and $C_{EL} = 1$ M. In this case, no desorption of protein from the drop surface was detected upon rinsing, which shows that a monolayer of irreversibly adsorbed protein molecules is formed at this lower protein concentration.

From these results, we can conclude that a protein monolayer is formed at 0.02 wt% BLG in the entire range of electrolyte concentrations studied. The observed increase of Γ at $C_{EL} > 50$ mM is due to formation of a more compact monolayer of protein molecules as a result of suppressed intra- and intermolecular electrostatic repulsion. At $C_{BLG} = 0.1$ wt%, a monolayer is formed at $C_{EL} <$ 50 mM, whereas a multilayer is formed when $C_{EL} \geq 150$ mM.

The effect of pH on Γ for emulsions stabilized by 0.02 wt% BLG at two electrolyte concentrations, $C_{EL} = 10$ and 150 mM, was studied. As seen from Figure 4, Γ passes through a maximum as a function of pH. Interestingly, we found that the adsorption is virtually the same for both electrolyte concentrations, Γ = 2.6 mg/m² at pH = 5.0 ≈ IEP, and is noticeably higher than that at natural pH = 6.2 (1.4 mg/m² for $C_{EL} = 150$ mM and 0.8 mg/m² for $C_{EL} = 10$ mM). The larger adsorption around the IEP is probably due to suppressed electrostatic repulsion between the protein molecules and, hence, to formation of a more compact adsorption layer. Similar dependencies are reported in the literature for BLG and for other globular proteins at oil−water and air−water interfaces.[5,6,19,20]

To check whether the higher value of Γ at pH = 5.0 is due to formation of a multilayer, we rinsed the emulsion formed at pH = 5.0 and $C_{EL} = 150$ mM with the respective electrolyte solution. We found that the initial adsorption of 2.6 mg/m² remained almost the same, 2.5 mg/m², after rinsing. This result shows that a more compact adsorption monolayer (no multilayer) is formed on the drop surface around the IEP. The latter conclusion is in qualitative agreement with the results obtained by Atkinson et al.[19] via the method of neutron reflectivity, who showed that the BLG adsorption at the air−water interface increases from 1.69 up to 2.45 mg/m² while reducing pH from 7.0 down to 5.74 ($C_{BLG} = 0.1$ wt% and $C_{EL} = 20$ mM). The authors[19] used a two-layer model to fit their experimental data for the structure of the adsorption layer at pH = 7.0, whereas a monolayer fit was used at pH = 5.74. These results were explained[19] by a tighter packing of the protein molecules in the adsorption monolayer at pH close to the IEP.

Away from the IEP, our experiments showed a lower adsorption at $C_{EL} = 10$ mM in comparison with the higher electrolyte concentration, $C_{EL} = 150$ mM, see Figure 4. The lower adsorption at $C_{EL} = 10$ mM is probably due to a more significant electrostatic repulsion between the protein molecules.

In conclusion, the protein adsorption passes through a maximum as a function of pH at 0.02 wt% BLG. This maximum is located around the IEP, corresponds to a compact monolayer of protein molecules, and its magnitude does not depend on C_{EL}. Lower adsorption is measured away from the IEP, and especially at lower electrolyte concentration, due to electrostatic repulsion between the protein molecules.

3.3. Coalescence Stability of Emulsions. *3.3.1. Dependence on Electrolyte Concentration.* The dependence of the critical osmotic pressure for coalescence, P_{OSM}^{CR}, on C_{EL} is presented in Figure 5 for the natural pH = 6.2. The stability of emulsions prepared with 0.02 wt% solutions of BLG (empty circles in Figure 5) passes through a maximum around $C_{EL} = 10$ mM. First, P_{OSM}^{CR} increases from 4 to 8 kPa when C_{EL} is increased from 1.5 to 10 mM. The additional increase of C_{EL} from 10 to 50 mM leads to a reduction of P_{OSM}^{CR} down to 5 kPa. The emulsion stability remains almost a constant, $P_{OSM}^{CR} \approx 3.5$ kPa, at higher electrolyte concentrations, $C_{EL} > 150$ mM.

For the emulsions prepared with 0.1 wt% BLG solutions (filled squares in Figure 5), the dependence of P_{OSM}^{CR} on

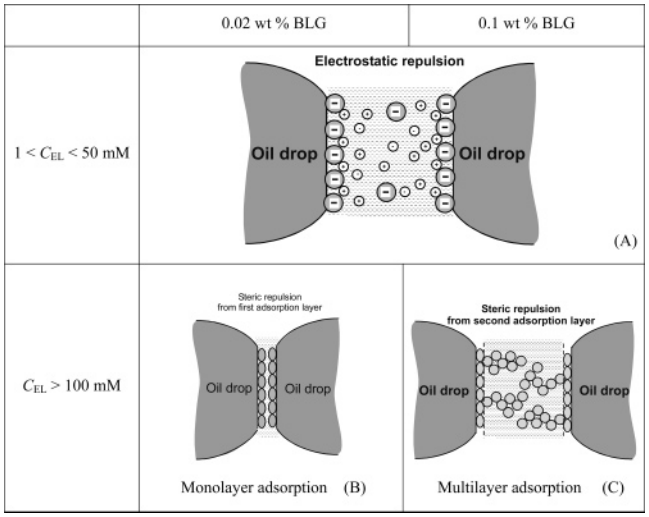

Figure 6. Schematic presentation of the main types of forces that govern the coalescence stability of BLG emulsions at natural pH = 6.2.

C_{EL} is different. At low and moderate electrolyte concentrations, $1.5 \leq C_{EL} \leq 50$ mM, the stability passes through a maximum, similarly to the emulsions prepared with 0.02 wt% BLG solution. However, at higher electrolyte concentrations, the emulsion stability increases from 7.5 up to 13 kPa when C_{EL} increases from 50 mM to 1 M. The stability of emulsions containing 0.1 wt% BLG is always higher than that at 0.02 wt% BLG at a given electrolyte concentration, especially at $C_{EL} > 50$ mM.

The qualitative explanation of the observed dependence of P_{OSM}^{CR} on C_{EL} is the following (see Figure 6): (1) At $C_{EL} < 100$ mM, the emulsion stability is governed by a significant electrostatic repulsion at both BLG concentrations studied. The quantitative comparison of the experimentally obtained and the theoretically calculated electrostatic barriers to drop−drop coalescence, presented in the subsequent Section 4, shows that the observed maximum in emulsion stability, at $C_{EL} \approx 10$ mM, corresponds to a maximum in the interdroplet electrostatic repulsion. (2) For emulsions prepared with 0.1 wt% BLG solutions, the observed significant increase in emulsion stability at $C_{EL} > 100$ mM is due to formation of a protein adsorption multilayer, which leads to an efficient steric stabilization of the emulsion films. (3) For emulsions prepared with $C_{BLG} = 0.02$ wt%, at $C_{EL} > 100$ mM, the emulsion stability is governed by a steric repulsion between adsorption monolayers on the drop surfaces, which ensures $P_{OSM}^{CR} \approx 3.5$ kPa independently of electrolyte concentration. Quantitative estimates of the interdroplet surface forces, confirming the occurrence of these three different cases in the studied emulsions, are presented in Section 4.

3.3.2. Dependence on pH of the Aqueous Phase. The effect of pH on emulsion stability was studied at $C_{BLG} = 0.02$ wt% and two different electrolyte concentrations, 10 and 150 mM (see Figure 7). The emulsion stability passes through a deep minimum at pH = 5.0 ≈ IEP, where the stability is practically the same at both electrolyte concentrations studied, $P_{OSM}^{CR} \approx 0.5$ kPa. Experiments performed at higher electrolyte concentrations, $C_{EL} = 300$ and 1000 mM, confirmed that the emulsion stability is independent of the electrolyte concentration at pH = IEP (results not shown in Figure 7). Measurements at higher protein concentration, 0.1 wt%, confirmed that the emulsion stability at pH = IEP = 5.0 was lower as compared to pH = 6.2 (3 kPa versus 10.7 kPa for emulsions containing 0.1 wt% BLG + 150 mM electrolyte).

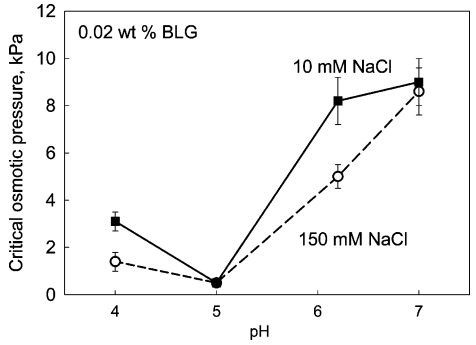

Figure 7. Critical osmotic pressure for coalescence, P_{OSM}^{CR}, as a function of pH in emulsions stabilized by 0.02 wt% BLG at two different electrolyte concentrations, $C_{EL} = 10$ mM (filled squares) and $C_{EL} = 150$ mM (open circles).

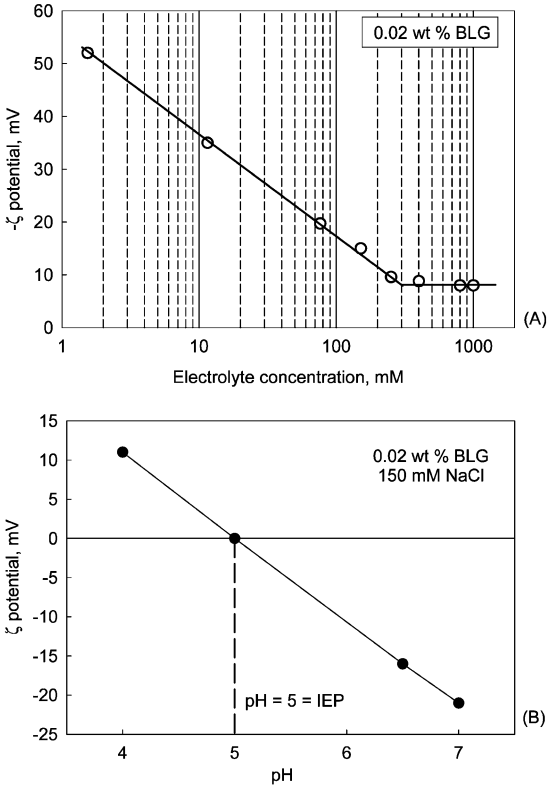

Figure 8. ζ-potential as a function of (A) electrolyte concentration at natural pH and (B) pH at $C_{EL} = 150$ mM. The emulsions are prepared at $C_{BLG} = 0.02$ wt%.

At pH away from the IEP, the stability of emulsions, prepared with 10 mM electrolyte solution, is higher (compared to 150 mM electrolyte) due to a pronounced electrostatic repulsion between the drops. At pH = 4.0, P_{OSM}^{CR} is around 3 times lower than that at natural pH = 6.2 at both electrolyte concentrations studied. The observed higher emulsion stability at pH = 6.2 can be explained qualitatively by the fact that the magnitude of the electrical drop-surface potential is higher as compared to pH = 4.0 (see Figure 8B) and, hence, the electrostatic repulsion between the drops is stronger.

Let us explain qualitatively what is the reason for the very low emulsion stability at pH = 5.0:

Note, first, that the protein adsorption is maximal, whereas the emulsion stability is minimal at pH = 5.0. In other words, the low coalescence stability at pH = 5.0, as compared to the natural pH = 6.2, cannot be explained by a reduced protein adsorption. These results are in good agreement with the data of Das and Kinsella.[5,6]

The suppressed electrostatic repulsion at pH around IEP can be suggested as another possible explanation for the lower emulsion stability under these conditions. However, the electrostatic repulsion is suppressed, as well, at the highest electrolyte concentration, $C_{EL} = 1$ M, at the natural pH = 6.2 (see the next section for the respective calculations), whereas the stability under these conditions, $C_{EL} = 1$ M and pH = 6.2, is much higher in comparison with pH = 5.0 (3.5 vs 0.5 kPa). Therefore, the suppressed electrostatic repulsion alone cannot explain the observed low emulsion stability at pH = 5.

Another possible explanation for the lower stability at pH = 5 could be the larger drop size of these emulsions. We found that the mean drop size, d_{32}, is around 1.5 times larger than that at natural pH (see Figure 2). An approximate estimate of the drop size effect on emulsion stability could be made by assuming that the dependence of the stability on d_{32} is similar to the dependence, obtained in ref 14 for the same system at $C_{EL} = 150$ mM, namely, that P_{OSM}^{CR} is approximately proportional to $1/d_{32}$. Under the latter assumption, we can estimate that a 1.5-fold increase of d_{32} should lead to about 1.5-fold decrease of P_{OSM}^{CR}, whereas we observe a 7-fold decrease in our experiments. Therefore, the drop-size effect cannot explain the very low emulsion stability observed at pH ≈ IEP.

The most probable explanation for the excessive decrease of emulsion stability at pH ≈ IEP is the formation of an adsorption protein layer of different structure, in comparison with the layers formed away from the IEP, when the protein molecules are charged. One possible explanation is that a relatively rigid adsorption layer is formed at pH ≈ 5.0, which behaves as a fragile/brittle shell. The formation of such fragile protein layers was reported[32] in experiments with emulsion films, stabilized by bovine serum albumin (BSA) close to the IEP of this protein—the authors of ref 32 showed by optical microscopy that the emulsion films are highly heterogeneous in thickness and easily rupture at pH = IEP = 5.2 (see Figure 9 in ref 32). Similar explanation for the effect of aging (long-term shelf-storage) on the coalescence stability of emulsions was suggested and discussed in ref 15.

4. Theoretical Estimates of the Barrier to Drop−Drop Coalescence and Comparison with the Experimental Results

The presentation of the theoretical estimates and their comparison with the experimental results is organized as follows.

First, we describe the procedure for calculating the electrostatic and van der Waals interactions, which are used to estimate theoretically the electrostatic barriers, Π_{MAX}, in the disjoining pressure isotherm at different electrolyte concentrations and natural pH = 6.2. In parallel, from the experimentally determined value of P_{OSM}^{CR}, we calculate the capillary pressure, P_{OI}^{CR}, which characterizes the stability of the emulsion films, intervening between the drops in the uppermost layer of the emulsion cream and the continuous oil layer, formed on top of the cream during centrifugation.

Afterward, the theoretically calculated electrostatic barriers, Π_{MAX}, are compared to the values of the critical capillary pressure, P_{OI}^{CR}, determined in the centrifugation experiments. This comparison shows that we could explain only the experimental results for low and moderate ionic strengths away from the IEP when assuming that the electrostatic and van der Waals interactions are significant. The electrostatic barrier disappears at high electrolyte concentration, $C_{EL} > 100$ mM, which means that other mechanisms of emulsion stabilization are operative. That is why the contribution of the steric repulsion is introduced into the total disjoining pressure isotherm to explain the emulsion stability at high electrolyte concentrations. The comparison of the respective theoretical estimates with the available experimental results shows that the combination of van der Waals, electrostatic, and steric interactions explains very well the results obtained at high BLG and electrolyte concentrations when protein adsorption multilayers are formed.

Table 1. Values of the Hamaker Constants between the Various Phases (w = water, o = oil, pr = protein layer) Used for Calculating the van der Waals Component of the Disjoining Pressure[36,37]

A_{132}	$A_{\nu=0} \times 10^{20}$, J (unscreened)	$A_{\nu>0} \times 10^{20}$, J
$A_{pr-w-pr}$	0.267	1.017
A_{o-pr-w}	0.004	−0.65
A_{o-pr-o}	0.002	0.96

4.1. Procedure for Calculation of the van der Waals and Electrostatic Interactions. The van der Waals interaction was estimated by using a three-layer model of the emulsion films, which includes a contribution from the adsorbed protein molecules on the film surfaces:[36,50]

$$\Pi_{VdW} = -\frac{1}{6\pi}\left(\frac{A_{pr-w-pr}}{h^3} - \frac{2A_{o-pr-w}}{(h+\delta)^3} + \frac{A_{o-pr-o}}{(h+2\delta)^3}\right) \quad (6)$$

Here h is the thickness of the water core of the film, δ is the thickness of the adsorbed protein layer ($\delta \approx 3.6$ nm in our case[48]), and A_{ijk} is the Hamaker constant of interaction of phase i with phase k through phase j. The variations in the electrolyte concentration affect the value of Π_{VdW} as a result of the screening of the zero-frequency component of the Hamaker constant, $A_{\nu=0}$.[50] This effect could be accounted for by using the formulas:[50]

$$A_{ijk} = A_{ijk,\nu} = 0 + A_{ijk,\nu>0} \quad (7)$$

$$A_{screened}(\kappa h) = A_{unscreened,\nu} = 0(1 + 2\kappa h)\exp(-2\kappa h) + A_{\nu>0} \quad (8)$$

To calculate the zero-frequency component of the Hamaker constant, we used the expression:[50]

$$A_{132,unscreened,\nu=0} = \frac{3}{4}k_B T\left(\frac{\epsilon_1 - \epsilon_3}{\epsilon_1 + \epsilon_3}\right)\left(\frac{\epsilon_2 - \epsilon_3}{\epsilon_2 + \epsilon_3}\right) \quad (9)$$

where ϵ_k is the static dielectric permittivity of phase k ($k = 1, 2, 3$). The values $\epsilon_W = 80$, $\epsilon_{PR} = 3$, and $\epsilon_{OIL} = 2.55$ were used in our estimates.[36,37] As seen from the calculated unscreened values of $A_{\nu=0}$ and $A_{\nu>0}$, presented in Table 1 (see also ref 36), the zero-frequency components of the Hamaker constants for the interactions oil−protein−water and oil−protein−oil, A_{o-pr-w} and A_{o-pr-o}, are negligible because the dielectric constants ϵ_{PR} and ϵ_{OIL} are very similar in magnitude.

To calculate the electrostatic component of the disjoining pressure, $\Pi_{EL}(h)$, we used the following expression, derived by Derjaguin et al.:[51]

$$\Pi_{EL} = 4n_0 k_B T \cot^2\theta, \quad \kappa h = 2F(\varphi,\theta)\sin\theta \quad (10)$$

(50) Israelachvili, J. N. *Intermolecular and Surface Forces*, 2nd ed.; Academic Press: New York, 1992; Chapters 11−14.

(51) Derjaguin, B. V.; Churaev, N. V.; Muller, V. M. *Surface Forces*, Plenum Press: New York, 1987.

where n_0 is the electrolyte number concentration, k_BT is the thermal energy, κ is the inverse Debye screening length, and $F(\varphi,\theta)$ is an elliptic integral of first kind. Under the assumption of *fixed electrical surface potential* of the drops, Ψ_S, the relation between φ and θ is[51]

$$\cos\varphi = \frac{\cot\theta}{\sinh\left(\frac{e\Psi_S}{2k_BT}\right)} \tag{11a}$$

where e is the elementary electrical charge. For *fixed surface charge*, the respective relation between φ and θ is[51]

$$\tan\varphi = \tan\theta\sinh\left(\frac{e\Psi_\infty}{2k_BT}\right) \tag{11b}$$

where Ψ_∞ is the value of Ψ_S at $h\rightarrow\infty$.

As seen from eqs 10 and 11, Π_{EL} depends on the electrolyte concentration and on the electrical surface potential, Ψ_S. In its own turn, Ψ_S depends mainly on the protein adsorption, electrolyte concentration, and pH.

To estimate the values of Ψ_S needed in the theoretical calculations of the electrostatic barrier, we used experimental data for the ζ-potential of the drops in the studied emulsions. The measured ζ-potentials for emulsions prepared with 0.02 wt% BLG solution at natural pH are presented in Figure 8A as a function of C_{EL}. The BLG molecules are negatively charged, and their ζ-potential decreases in magnitude from -52 to -15 mV, while C_{EL} increases from 1.5 to 150 mM. For estimates of the electrostatic repulsion in the emulsion films, we used the following empirical formula to interpolate the measured values of the ζ-potential (see Figure 8A):

$$\zeta = -55.4 + 18.9\log C_{EL};\quad 1.5\text{ mM} \le C_{EL} \le 150\text{ mM} \tag{12}$$

where the ζ-potential is expressed in millivolts and C_{EL} is expressed in millimoles. At higher electrolyte concentrations, C_{EL} between 250 and 1000 mM, the ζ-potential is almost constant, -9 ± 2 mV, and this value is used in the following calculations for $C_{EL}\ge250$ mV.

The dependence of the ζ-potential on pH for emulsions with $C_{EL}=150$ mM is presented in Figure 8B. It is seen that the ζ-potential is virtually zero at pH = 5.0 $\approx$ IEP. The BLG molecules are positively charged at pH = 4.0 and negatively charged at pH = 6.2. The obtained pH dependence of the ζ-potential is in a good agreement with literature data for BLG.[12]

In principle, the ζ-potential could depend on protein concentration. To check this effect, we compared the ζ-potential for emulsions prepared with BLG solutions of 0.02 and 0.1 wt% at $C_{EL}=1.5$ mM and natural pH. The measured values of the ζ-potential were -52 and -54 mV, respectively, which is in the framework of our experimental accuracy. This lack of dependence on the protein concentration (in the studied range) is probably due to the fact that an almost dense adsorption layer is formed at 0.02 wt% BLG and the further increase of C_{BLG} does not affect significantly the protein adsorption and the ζ-potential (at electrolyte concentrations below 50 mM). For this reason, in the following estimates, we do not consider the possible effect of the BLG concentration on the ζ-potential.

To estimate Ψ_S from the measured ζ-potentials, we assumed that the distance δ_S between the so-called "shear plane", in which the ζ-potential is measured, and the outer Helmholtz plane, in which Ψ_S is defined (see, e.g., ref 52), did not depend on electrolyte concentration in the studied emulsions. Thus, we could calculate Ψ_S from the experimental value of ζ (measured at the respective pH and electrolyte concentration) by using the Poisson–Boltzmann equation and a specified value of δ_S. To find the most appropriate value of δ_S, we compared the theoretical electrostatic barriers at various NaCl concentrations, calculated with one and the same value of δ_S, with the results for the coalescence stability obtained in the centrifugation experiments at natural pH = 6.2. In these calculations, the value of δ_S was varied in the range between 0 and 0.58 nm (twice the diameter of the water molecules) because measurements with a surface-force apparatus showed that δ_S is no larger than one to two molecular diameters.[50] The comparison of the theoretical barriers and the experimental results demonstrated that one and the same conclusions are reached while δ_S was varied within the specified range irrespectively of the concrete value of δ_S. Moreover, the best agreement between the theoretical barriers and the results from the coalescence experiments was obtained with $\delta_S\approx0$ (i.e., shear plane placed very close to the outer Helmholtz plane), which corresponds to $\Psi_S\approx\zeta$. For these reasons, only the estimates with $\Psi_S\approx\zeta$ are presented and discussed below.

Summarizing this section, we calculate the van der Waals component of disjoining pressure by assuming a three-layer model, which accounts for the contribution of the adsorbed protein molecules on the film surfaces. The screening of the zero-frequency component of the Hamaker constant by the electrolyte dissolved in the aqueous phase is explicitly taken into account. The electrostatic component of the disjoining pressure is calculated by solving the Poisson–Boltzmann equation numerically and by assuming that the surface potential of the single drops is equal to the measured ζ-potential. The disjoining pressure in the emulsion films is considered as a superposition of van der Waals and electrostatic contributions only (the contribution of the steric repulsion is considered later):[50−52]

$$\Pi_{TOT} = \Pi_{VdW} + \Pi_{EL} \tag{13}$$

where Π_{VdW} and Π_{EL} are calculated from eqs 6 and 10, respectively. From the calculated $\Pi(h)$ isotherms, we determine the height of the electrostatic barrier, Π_{MAX}. The latter is compared in Section 4.3 with the experimentally determined values of P_{OI}^{CR}.

4.2. Determination of the Critical Capillary Pressure, P_{OI}^{CR}. To make a proper comparison between theory and experiment, we need an appropriate pressure, determined from the centrifugation data, which has to be compared with the theoretical value of the coalescence barrier, Π_{MAX}.

Previous studies[14,53] showed that the coalescence in emulsions could occur by two different modes: (1) As a coalescence of the drops in the uppermost layer of the emulsion cream with an already released bulk layer of oil (or macroscopic oil lens)—see Figure 9 for the configuration of the system under discussion. This mode of coalescence is termed "drop-large phase coalescence".[53] (2) By a drop–drop coalescence inside the cream, which leads to forma-

(52) Kralchevsky, P. A.; Danov, K. D.; Denkov, N. D. Chemical physics of colloid systems and interfaces. In *Handbook of Surface and Colloid Chemistry*; Birdi, K. S., Ed.; CRC Press LLS: Boca Raton, 1997; Chapter 11.

(53) Denkov, N. D.; Tcholakova, S.; Ivanov, I. B.; Campbell, B. Methods for evaluation of emulsion stability at a single drop level. In *Third World Congress on Emulsions,* Lyon **2002**, Paper No 198.

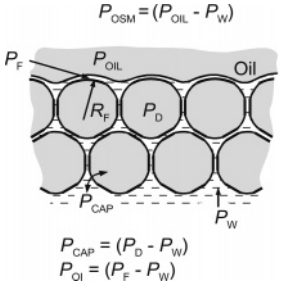

Figure 9. Schematic presentation of the uppermost layer of an emulsion in contact with continuous oil layer.

tion of much larger drops that coalesce with each other afterward to release the continuous oil phase on top of the cream.

In a previous study,[53] we showed that, with respect to the driving pressure for film thinning, the films formed between two oil drops inside the cream should be less stable than the films formed between the oil drops and the continuous oil phase. The reason is that the driving pressure for film thinning between two equally sized drops (which is the capillary pressure of the drops, $P_{CAP} = P_D - P_W$) is higher than the pressure squeezing the emulsion film between an oil drop and the neighboring large oil phase, $P_{OI} = P_F - P_W$ (see Figure 9). Therefore, with respect to the driving pressure, the coalescence through mode 2 would be more favored. However, with respect to the film size, the prevailing mode for emulsion destabilization should be the coalescence between a drop and the continuous oil phase, i.e., mode 1, because the respective emulsion film is larger in diameter than the film between two equally sized drops.[53] It is not known in advance which of these two effects would prevail in a given system and what would be the actual mode of emulsion collapse.

By following the experimental procedure described in Section 3.5 of ref 14, we found that the prevailing mechanism in the emulsions formed at natural pH = 6.2 and $C_{EL} \leq 300$ mM was the drop-large phase coalescence (mode 1). That is why in this section we calculate, from the experimental data about emulsion coalescence stability (obtained by centrifugation), the critical capillary pressure, P_{OI}^{CR}, which corresponds to the rupture of the emulsion films between the oil drops and the bulk oil layer at the top of the emulsion cream. In the next subsection, we compare the values of P_{OI}^{CR} with Π_{MAX}.

The capillary pressure, P_{OI}, driving the thinning of the film which is formed between an oil drop in the uppermost layer of the emulsion column and the adjacent large oil phase, see Figure 9, is given by the expression:[54,55]

$$P_{OI} = P_F - P_W = P_{OIL} - P_W + \frac{2\sigma_{OW}}{R_F} \qquad (14)$$

where P_F is the pressure in this film and R_F is its radius of curvature. P_{OIL} is the pressure in the oil phase above the drop, whereas P_W is the pressure in the aqueous phase of the emulsion. As shown by Princen[56] the pressure difference, $P_{OIL} - P_W$, is equal to the osmotic pressure of the emulsion, P_{OSM}. On the other hand, from the Laplace equation of capillarity, one can express the last term in eq 14:[55]

$$\frac{2\sigma_{OW}}{R_F} = \frac{1}{2}(P_D - P_{OIL}) \qquad (15)$$

Thus combining eqs 14−15 and taking into account that $P_{CAP} = P_D - P_W$, one obtains

$$P_{OI} = \frac{1}{2}(P_{OSM} + P_{CAP}) = \frac{P_{OSM}(1 + f(\Phi))}{2f(\Phi)} \qquad (16)$$

where P_{OSM} is the emulsion osmotic pressure at the top of the cream, P_{CAP} is the capillary pressure of the oil drops in the uppermost layer, and $f(\Phi)$ is the fraction of the interface between the emulsion and the neighboring continuous oil phase which is occupied by films. To write the last expression in eq 16, we used the relationship between P_{OSM} and P_{CAP} theoretically established by Princen:[49]

$$P_{CAP} = \frac{P_{OSM}}{f(\Phi)} \qquad (17)$$

For relatively high oil volume fractions at the top of the cream, Φ, (i.e., at $\Phi > 0.975$), the following relation was found[49] to describe the experimental data for polydisperse oil-in-water emulsions:

$$f(\Phi) = (1 - 1.892(1 - \Phi)^{1/2})^2 \qquad (18)$$

To evaluate the critical oil volume fraction, Φ_{CR}, at which the bulk oil layer is released on top of the emulsion cream in our centrifugation experiments, we used the experimental values of P_{OSM}^{CR} (see Section 2.5 and eq 4) and the empirical relation between the dimensionless osmotic pressure, $\tilde{P}_{OSM}$, and Φ, proposed by Princen:[49]

$$\tilde{P}_{OSM} = 0.5842\frac{(1 - 1.892(1 - \Phi)^{1/2})^2}{(1 - \Phi)^{1/2}} \qquad (19)$$

where the dimensionless osmotic pressure is defined as[49]

$$\tilde{P}_{OSM} = P_{OSM}(R_{32}/\sigma_{OW}) \qquad (20)$$

R_{32} is the mean volume-surface radius (measured microscopically, $R_{32} = d_{32}/2$), and σ_{OW} is the oil−water interfacial tension.

Equations 16−20 allow us to determine P_{OI}^{CR} from the available experimental data. Briefly, the numerical procedure is as follows. P_{OSM}^{CR}, determined by centrifugation, is introduced in eq 20 to calculate the dimensionless critical osmotic pressure, $\tilde{P}_{OSM}^{CR}$. The latter is used in eq 19 to estimate Φ_{CR}, which in turn is used to determine $f(\Phi_{CR})$ from eq 18. Finally, the value of $f(\Phi_{CR})$ is used for calculation of P_{OI}^{CR} from eq 16.

4.3. Comparison of Π_{MAX} (Calculated from DLVO Theory) with P_{OI}^{CR}. The points in Figure 10 show the experimentally determined values of P_{OI}^{CR} vs C_{EL} at pH = 6.2 and $C_{BLG} = 0.02$ wt%, whereas the dashed curve shows the theoretically calculated dependence of Π_{MAX} on C_{EL} (constant surface potential is assumed to plot this curve, eq 11a). One sees that the theoretical dependence of Π_{MAX} on C_{EL} follows very well the trend of the experimental points for $C_{EL} < 80$ mM—the theoretical curve passes through a maximum at $C_{EL} \approx 15$ mM, just as the experimental points do. The initial increase of Π_{MAX}, when

(54) Hadjiiski, A.; Tcholakova, S.; Denkov, N. D.; Durbut, P.; Broze, G.; Mehreteab, A. Effect of oil additives on foamability and foam stability: 2. Entry barriers. *Langmuir* **2001**, *17*, 7011.

(55) Hadjiiski, A.; Tcholakova, S.; Ivanov, I. B.; Gurkov, Th. D.; Leonard, E. F. Gentle film trapping technique with application to drop entry measurements. *Langmuir* **2002**, *18*, 127.

(56) Princen, H. M. Pressure/volume/surface area relationships in foams and highly concentrated emulsions: Role of volume fraction. *Langmuir* **1988**, *4*, 164.

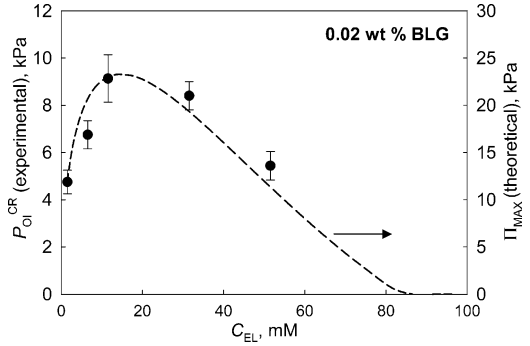

Figure 10. Experimentally determined dependence of the critical capillary pressure, P_{OI}^{CR}, on C_{EL} for emulsions stabilized by 0.02 wt% BLG along with the theoretical dependence of Π_{MAX} vs C_{EL} from the DLVO theory (dashed curve). The points are associated with the left-hand-side ordinate, whereas the curve is associated with the right-hand-side ordinate (see the text for additional explanations).

C_{EL} increases from 1.5 up to 10 mM, is due to the increase of ion concentration in the aqueous solution, n_0, which in turn leads to stronger electrostatic repulsion, despite the decrease of the electric surface potential and the Debye length, κ^{-1} (see eqs 10−11 and Figure 8 above). The subsequent decrease of Π_{MAX} at $C_{EL} > 15$ mM is due to the decrease of the surface potential, Ψ_S, which is the prevailing effect at moderate and high electrolyte concentrations.

It is known from the literature[50,51] that the boundary condition of constant surface potential corresponds to the weakest electrostatic repulsion whereas the boundary condition of constant surface charge corresponds to the strongest electrostatic repulsion between charged surfaces. The charge-regulation boundary condition is between these two limiting cases. Our theoretical calculations showed that the electrostatic repulsion between the drops is overwhelmed by the van der Waals attraction at $C_{EL} \geq 85$ mM, if one assumes a boundary condition of constant surface potential in the DLVO theory—see eq 11a and the dashed curve in Figure 10. Above this electrolyte concentration, the disjoining pressure is attractive at arbitrary film thickness, h. Similarly, we found that the theoretically calculated electrostatic barrier disappears at $C_{EL} \geq 100$ mM, if we assume a constant surface charge, eq 11b (the respective theoretical curve is not shown in Figure 10). One can conclude from these estimates that the electrostatic repulsion is operative only for emulsions with $C_{EL} < 100$ mM, independently of the assumed boundary condition (constant potential, constant charge, or charge regulation). Therefore, the emulsion stability at higher electrolyte concentrations, $C_{EL} \geq 100$ mM, is determined by other factors (see Section 4.4 below).

Let us compare the magnitudes of Π_{MAX} and P_{OI}^{CR} for the emulsions with $C_{EL} < 100$ mM, see Figure 10. As mentioned above, the shape of the theoretical curve for Π_{MAX} reproduces well the experimentally observed trend of P_{OI}^{CR} vs C_{EL}. However, the values of P_{OI}^{CR} are around 2.5 times smaller in magnitude than Π_{MAX}—note that the experimental points in Figure 10 correspond to the left-hand axis, whereas the theoretical curve corresponds to the right-hand axis and both axes are scaled by a factor of 2.5 with respect to each other. Several possible explanations for the observed difference between the values of P_{OI}^{CR} and Π_{MAX} are briefly discussed in the following paragraphs.

In the centrifugation experiments, the volume fraction of the oil drops gradually increases at the top of the emulsion cream under the action of the centrifugal acceleration. This process of drop compaction and enhanced drop deformation is accompanied with an expansion of the drop surface. As a result, the protein adsorption on drop surface should decrease unless additional protein adsorbs to compensate for the expanded interfacial area. The diffusion of dissolved protein inside the emulsion films, formed between the deformed drops, could be too slow to ensure sufficiently fast adsorption due to the fact that these films are only few nanometers thick and because the protein molecules should travel long distances from the Plateau borders toward the film center. Hence, one could expect that the values of protein adsorption and surface charge density decrease, as compared to those before centrifugation. The reduced surface charge density would correspond to a lower electrostatic barrier in comparison with that calculated by the procedure described in Section 4.1. One indication that this effect could be significant is the experimental fact that the stability of emulsions, containing 0.1 wt% BLG, is around 50% higher than that for emulsions stabilized by 0.02 wt% BLG, see Figure 5. One can explain this result by assuming that the higher BLG concentration results in a faster protein adsorption during surface expansion.

One should note, however, that the maximum surface expansion in the process of drop deformation, starting from spherical drops before centrifugation up to deformed polyhedra with volume fraction $\Phi \rightarrow 1$ at high centrifugal accelerations, is only by about 8%.[49] Therefore, the respective decrease of the surface charge density in the process of drop deformation is expected to be about or smaller than 8%. Such a moderate decrease of surface charge density could not explain entirely the observed 2-fold difference between the experimental data and the theoretical estimate of the electrostatic barrier by the DLVO theory. However, the surface expansion could lead to formation of spots on the film surfaces, which are deprived of adsorbed protein—such "bare" spots are expected to lead to a hydrophobic attraction in the emulsion film (not accounted for in the DLVO theory), which would facilitate the film destabilization.[57]

Another possible explanation for the observed difference between Π_{MAX} and P_{OI}^{CR} is a theoretical overestimate of the electrostatic repulsion by the DLVO theory. Similar explanation for an observed discrepancy between theoretical estimates and experimental results for the electrostatic barriers in foam films stabilized by SDS was suggested in ref 58. In ref 58, the disjoining pressure isotherm, $\Pi(h)$, the film electrical conductance, and the surface tension isotherms were measured. The authors found[58] that, at low electrolyte concentration, the surface charge density needed to fit the experimentally measured $\Pi(h)$ isotherm was significantly lower than the charge density estimated from the measured surface tension isotherms and foam film conductance. In recent experiments, Ivanov et al.[59] confirmed that a significant discrepancy is observed between the DLVO theory and the experimental isotherms $\Pi(h)$ for SDS-stabilized foam

(57) Angarska, J. K.; Dimitrova, B. S.; Danov, K. D.; Kralchevsky, P.; Ananthapadmanabhan, K. P.; Lips, A. Detection of the hydrophobic surface force in foam films by measurements of the critical thickness of film rupture. *Langmuir* **2004**, *20*, 1799.

(58) Yaros, H. D.; Newman, J.; Radke, C. J. Evaluation of DLVO theory and disjoining-pressure and film-conductance measurements of common-black films stabilized by sodium dodecyl sulfate. *J. Colloid Interface Sci.* **2003**, *262*, 442.

(59) Ivanov, I. B.; Basheva, E.; Danov, K. D.; Gurkov, T. D.; Ananthapadmanabhan, K. P.; Lips, A. Discrete charge model of thin films, stabilized by ionic surfactants. Presentation at the Conference on Physics and Design of Foams; July 22−23, 2004, Edgewater, NJ.

films, when the film thickness becomes similar or smaller than the inverse Debye screening length, $\kappa h \leq 1$. The observed discrepancy was explained by Ivanov and coworkers by considering the discrete character of the actual charges on the film surfaces—an effect which is neglected in the DLVO theory and seems to be insignificant at large film thickness, $\kappa h > 1$, but appears to be important at small film thickness (up to several times difference was measured between the experimental data for $\Pi(h)$ and the corresponding theoretical values, calculated from the DLVO model).

As seen from Figure 10, the DLVO theory adequately describes, at least qualitatively, the observed trends in the emulsion stability vs C_{EL} at low and moderate electrolyte concentrations. Therefore, we can conclude that the stability of BLG emulsions at $C_{EL} < 100$ mM is mainly governed by electrostatic repulsion, acting between the drop surfaces covered by protein monolayers. On the other hand, the electrostatic repulsion could not explain the observed emulsion stability at $C_{EL} > 100$ mM because the electrostatic barrier disappears due to the low ζ-potential and the short Debye screening length, κ^{-1}, at such high electrolyte concentrations.

The experimental results in Figure 5 show that, at $C_{EL} > 100$ mM, the stability of emulsions containing 0.1 wt% BLG is much higher than the stability of emulsions containing 0.02 wt% protein. Moreover, P_{OI}^{CR} remains almost constant for emulsions with $C_{BLG} = 0.02$ wt% while varying the electrolyte concentrations, whereas P_{OI}^{CR} rapidly increases with C_{EL} for emulsions prepared with 0.1 wt% BLG solutions. These differences indicate that the emulsion stability is governed by different factors for $C_{BLG} = 0.02$ and 0.1 wt%, at high electrolyte concentrations.

As discussed in Section 3.2, the protein adsorption at 0.02 wt% BLG corresponds to a monolayer, whereas a multilayer is formed at $C_{BLG} = 0.1$ wt%. A simple theoretical model, taking into account the steric repulsion between the adsorbed protein multilayers, is presented in the next subsection for the emulsions prepared at $C_{BLG} = 0.1$ wt% and $C_{EL} > 100$ mM.

At the present moment, we have no quantitative approach to describe emulsion stability in the case of a monolayer adsorption and suppressed electrostatic repulsion (i.e., at $C_{BLG} = 0.02$ wt% and $C_{EL} > 100$ mM). The experimental data from Figure 5 show that the coalescence barrier is almost constant in these systems, 4 ± 1 kPa. We assume that, under these conditions, there is a direct contact between the protein monolayers adsorbed on the two opposite surfaces of the emulsion films because there are no long-range forces present. The factors that determine the stability of such emulsions are not well understood. One may expect that the emulsion film rupture and the subsequent drop coalescence in these systems are related to expansion of the drop surface (as a result of drop deformation or thermal fluctuations of film surface), with a possible formation of defects in the protein adsorption layers. This picture of film rupture suggests that the following types of factor could control emulsion stability in such systems: rheological properties of the protein adsorption layer (e.g., surface yield stress, elasticity, and/or viscosity), conformational state of the adsorbed protein molecules, and possibility for formation of inter- and intramolecular bonds.

4.4. Long-Ranged Steric Repulsion. The increased stability of the emulsions at $C_{BLG} = 0.1$ wt% and $C_{EL} > 100$ mM (in comparison with the stability predicted by DLVO theory) can be explained with a steric repulsion between the protein adsorption multilayers formed under these conditions. We emphasize that the model of steric repulsion described below has mainly illustrative purpose. Its aim is to demonstrate that one could explain the experimental results at high protein and electrolyte concentrations by a relatively simple, semiquantitative consideration of the steric repulsion. We do not claim that the model accounts accurately for the detailed structure of the adsorption layers and for the exact $\Pi(h)$ dependence.

In the literature, a large number of theoretical models for the steric repulsion between polymer layers can be found.[50,52,60−62] These models differ mainly in the assumed type of solvent−polymer interactions and in the complexity of calculations involved. It was shown in ref 63 that an expression derived originally by Dolan and Edwards[60] for the so-called "theta-solvents" can be used to describe reasonably well the data obtained with thin emulsion films, stabilized by BLG:

$$\Pi_{ST} = \frac{36\Gamma_T k_B T}{L} \exp(-h/L) \qquad (21)$$

where L is the characteristic distance of steric repulsion (for polymer chains it is equal to their radius of gyration, R_g) and Γ_T is the number density of chains per unit area of the adsorption layer. Equation 21 is derived under the assumption for a relatively low surface coverage by the polymer chains, so that each chain interacts independently with the chains attached to the opposite surface.[50,60]

The $\Pi(h)$ isotherm for emulsion films of type oil−water−oil, stabilized by 0.2 wt% BLG, was measured in ref 63. Hexadecane was used as an oil phase, the electrolyte concentration was fixed at 0.15 M, and pH = 6.2 was natural. The best fit of the measured $\Pi(h)$ isotherm by superimposing the van der Waals, electrostatic, and steric interactions gave $L = 9.8$ nm.[63] In an independent experimental study with BSA stabilized films, Dimitrova et al.[31] reported similar values for L. Such relatively large experimental values of L, in comparison with the protein dimensions ($\delta = 3.6$ nm for BLG), could be explained by assuming that the steric repulsion is either due to protein aggregates adsorbed on the film surfaces or to long protein tails protruding from partially denatured molecules. We assume in the further consideration that the long-ranged steric repulsion in our BLG emulsions is created by adsorbed protein aggregates, see Figure 6C. As shown below, the model based on this assumption describes very well the experimental data for the coalescence stability of the studied emulsions.

To develop a quantitative model, we suppose that only the protein aggregates adsorbed in the second adsorption layer (which is not in a direct contact with the oil−water interface) contribute to the long-ranged steric repulsion. In other words, we consider the first adsorption layer of protein molecules as a substrate over which chains of protein aggregates are attached, see Figure 6C. To avoid the necessity of introducing any unknown adjustable parameters in the model, we make the simplifying assumption that the protein aggregates can be modeled as linear chains formed by reversible aggregation of protein molecules (Figure 6C). Under these assumptions, we can estimate the number concentration of the protein ag-

(60) Dolan, A. K.; Edwards, S. F. Theory of the stabilization of colloids by adsorbed polymer. *Proc. R. Soc.* (*London*) **1974**, *A337*, 509.

(61) De Gennes, P. G. Polymers at an interface: a simplified view. *Adv. Colloid Interface Sci.* **1987**, *27*, 189.

(62) Semenov, N.; Joanny, J.-F.; Johner, A.; Bonet-Avalos, J. Interaction between two adsorbing plates: The effect of polymer chain ends. *Macromolecules* **1997**, *30*, 0, 1479.

(63) Dimitrova, T. D.; Vassileva, N.; Campbell, B. Manuscript in preparation.

gregates, Γ_T, from the experimental data for protein adsorption, Γ, by using the following equation:

$$\Gamma_T = (\Gamma - \Gamma_M)/N \tag{22}$$

where $\Gamma_M = 1.5$ mg/m^2 $= 49 \times 10^{-3}$ molecules/nm^2 is the protein adsorption in the first adsorption monolayer and N is the average number of protein molecules per one aggregate (one chain). The value of N can be approximately estimated by assuming that the protein aggregates have a structure similar to that of polymer chains in theta-solvent and that the single protein molecules play the role of the segments in a polymer chain. Thus, one can write[50]

$$L = R_g = \delta\sqrt{\frac{N}{6}} \tag{23}$$

where the effective length of the polymer segments is accepted to be equal to the diameter of the protein molecules, δ. For $L = 9.8$ nm (taken from ref 63) and $\delta = 3.6$ nm, one obtains $N = 44$ molecules per aggregate for 0.2 wt% BLG solution.

The fact that the mean number of protein molecules assembled in one protein aggregate could vary with the bulk protein concentration can be accounted for by using the thermodynamic theory of self-assembly. The latter predicts that the average aggregation number for linear aggregates is proportional to the square root of the bulk concentration:[50]

$$\frac{N(C_1)}{N(C_2)} = \left(\frac{C_1}{C_2}\right)^{1/2} \tag{24}$$

From eqs 22−24, we are able to determine all necessary parameters for calculating the contribution of the steric repulsion into the disjoining pressure isotherm, eq 21.

Briefly, the numerical procedure is the following. At given protein concentration, we calculate the number of protein molecules per aggregate, N, via eq 24 (assuming that $N = 44$ at $C_{BLG} = 0.2$ wt%) and the range of steric repulsion, L, from eq 23. From the experimentally measured protein adsorption, Γ, we estimate the surface density of protein aggregates, Γ_T, by using eq 22. The values of Γ_T and L are finally introduced into eq 21 to calculate the contribution of steric repulsion into the total disjoining pressure isotherm, $\Pi_{TOT}(h)$, which is considered as a superposition of steric, electrostatic (eq 10), and van der Waals (eq 6) interactions:

$$\Pi_{TOT} = \Pi_{VdW} + \Pi_{EL} + \Pi_{ST} \tag{25}$$

4.5. Comparison of P_{OI}^{CR} with Π_{MAX}, Calculated by Including Steric Repulsion. In this subsection, we compare the theoretically calculated maximums in the disjoining pressure isotherms, Π_{MAX} (including steric repulsion), with the experimental results for the emulsion coalescence stability obtained at $C_{BLG} = 0.1$ wt% and $C_{EL} \geq 150$ mM. To make this comparison as complete as possible, the experimental results presented in the previous sections are complemented with data for P_{OI}^{CR} and Γ, described in ref 14, for $C_{BLG} = 0.08$ wt% and $C_{EL} = 150$ mM.

The calculated parameters characterizing the steric interaction, the barriers in the disjoining pressure isotherm, Π_{MAX}, and the experimentally determined values of P_{OI}^{CR} are presented in Table 2. As seen from the last two columns in Table 2, the values of Π_{MAX} and P_{OI}^{CR} agree reasonably well (the difference is equal or smaller than 15%) for all studied BLG concentrations without using any adjustable parameter in the calculations. This comparison illustrates that the observed significant increase in emulsion stability at high electrolyte and protein concentrations, see Figure 5, can be explained with a steric repulsion between adsorbed protein aggregates.

Table 2. Comparison of Theoretically Calculated Values of the Electrostatic Barrier in the Disjoining Pressure Isotherm, Π_{MAX}, with Experimentally Determined Values of P_{OI}^{CR} at Different Protein and Electrolyte Concentrations at Natural pH = 6.2[a]

C_{EL} mM	C_{BLG} wt%	Γ mg/m^2	R_g nm	N	$\Gamma_T \times 10^3$ nm^{-2}	Π_{MAX} kPa	P_{OI}^{CR} kPa
150	0.08[b]	2.5 ± 0.3	7.79	28	1.14	6.8	8.0 ± 1.0
	0.1	3.0 ± 0.5	8.24	31	1.55	10.5	10.7 ± 0.5
300	0.1	3.2 ± 0.8	8.24	31	1.8	12.3	12.7 ± 1.0
1000	0.1	4.0 ± 0.8	8.24	31	2.2	15.3	13.8 ± 1.0

[a] Γ is experimentally determined protein adsorption; R_g is calculated radius of gyration of the protein aggregates; N is average number of protein molecules per one aggregate; Γ_T is the number surface concentration of protein aggregates. [b] Data taken from ref 14.

5. Conclusions

The effects of electrolyte concentration, C_{EL}, protein concentration, C_{BLG}, and pH on the mean drop size after emulsification, protein adsorption, and coalescence stability of BLG-containing emulsions were studied. The main experimental results can be summarized as follows.

(1) The mean drop size, d_{32}, depends very slightly on C_{EL} for emulsions prepared at natural pH = 6.2. The mean size is almost the same for both studied BLG concentrations, 0.02 and 0.1 wt%. The main reason for this slight dependence of d_{32} on C_{BLG} and C_{EL} is that the drop−drop coalescence during emulsification is negligible in these systems.

(2) The effect of pH on d_{32} is stronger than the effect of C_{EL}. A well-pronounced maximum in the dependence d_{32} vs pH is observed as a result of intensive drop−drop coalescence at pH around the protein isoelectric point (IEP ≈ 5.0). The drop coalescence is explained by a suppressed electrostatic repulsion and ineffective steric repulsion at pH ≈ IEP.

(3) At low electrolyte concentration, $C_{EL} < 50$ mM, and natural pH = 6.2, the protein adsorption Γ corresponds to a monolayer with a significant mean distance between the protein molecules at both BLG concentrations studied (0.02 and 0.1 wt%). At higher electrolyte concentration, $C_{EL} > 50$ mM, Γ increases due to formation of more compact adsorption monolayer when $C_{BLG} = 0.02$ wt%. In contrast, an adsorption protein multilayer is formed at high electrolyte and protein concentrations, $C_{EL} > 100$ mM and $C_{BLG} = 0.1$ wt%, as a result of suppressed electrostatic repulsion between the protein molecules in the adsorption layer.

(4) Protein adsorption passes through a maximum, as a function of pH, for emulsions stabilized by 0.02 wt% BLG at $C_{EL} = 150$ mM. The maximal adsorption is obtained at pH ≈ IEP due to suppressed electrostatic repulsion between the protein molecules. This adsorption corresponds to a monolayer.

A theoretical analysis is performed to clarify the relative contributions of the main types of surface forces governing emulsion stability—van der Waals, electrostatic, and steric. This analysis shows that

(1) The electrostatic interaction is important at both BLG concentrations studied, 0.02 and 0.1 wt%, if pH is

away from the IEP and $C_{EL} < 100$ mM. The coalescence stability of the respective emulsions is governed mainly by electrostatic and van der Waals forces.

(2) If the protein adsorbs as a multilayer ($C_{BLG} \geq 0.08$ wt% and $C_{EL} \geq 150$ mM), one should take into account the contribution of the steric repulsion, along with the van der Waals and electrostatic interactions.

(3) If the protein adsorption corresponds to a monolayer, Γ_M, and the electrostatic repulsion is suppressed, the emulsion stability does not depend significantly on electrolyte concentration (but depends on pH).

(4) Thus, we distinguish the following, qualitatively different cases, see Figure 6: (1) electrostatically stabilized emulsions with monolayer adsorption, (2) emulsions stabilized by a steric repulsion created by protein adsorption multilayers, and (3) emulsions stabilized by a steric repulsion created by adsorption monolayers. The coalescence stability of emulsions type 1 can be reasonably well described by DLVO theory. The stability of emulsions type 2 is described by a simple model, which accounts for the steric + DLVO interactions. Further experimental and theoretical efforts are needed to reveal the main factors that determine the stability of emulsions of type 3.

Although the emulsions studied in the current paper differ from the typical food emulsions by their larger mean drop size and lower protein concentration in the initial solution (prior to emulsification), the obtained results are probably relevant to many systems of practical interest. Indeed, by choosing appropriate protein concentrations in our experiments, C_{BLG}^{INI}, we ensured protein adsorption, Γ, similar to that in the systems of practical interest (see eq 3 for the relation between Γ, d_{32}, and C_{BLG}^{INI}). Since the emulsion coalescence stability depends primarily on the structure and properties of the protein adsorption layers, we expect that the observed effects of pH and electrolyte concentration on the protein adsorption and emulsion stability, as well as the discussed mechanisms of emulsion stabilization by BLG, are typical for emulsions containing globular proteins. The more trivial effect of the mean drop size on emulsion stability at a fixed value of Γ can be quantified as explained in refs 14−15, where we showed experimentally that the critical pressure for emulsion decay was inversely proportional to d_{32}.

Acknowledgment. Dr. K. Marinova, Mr. N. Hristov, and Mrs. D. Dimitrova from Sofia University are gratefully acknowledged for performing the interfacial tension and ζ-potential measurements. The authors of ref 63 are acknowledged for the permission to use their results prior to publication.

LA046891W